Simulating the viscoelastic response of the spinal cord

Nina Kristine Kylstad[1]

[1]Faculty of Mathematics and Natural Sciences
University of Oslo

10$^{\text{th}}$ June, 2014

Outline

- Medical backgound
- Simulation scenario
- Mathematical models
- Discretization
- Implementation
- Simulation results
- Conclusions

Outline

The Chiari I malformation

- Malformation of the brain / skull.
- Characterized by downward displacement of hindbrain:
  - 3 – 5mm below the base of the skull
  - May block CSF flow from brain to spinal column.
- Approximately 1% of normal adults have the malformation.
- Few display symptoms.

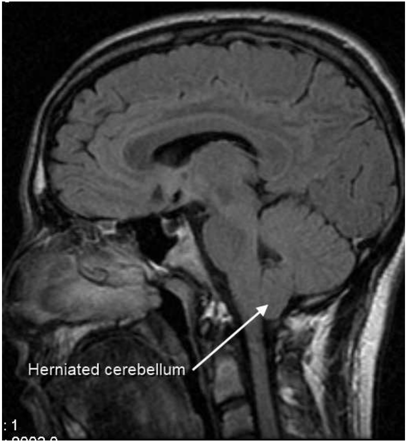

The Chiari I malformation

Common symptoms

Symptom	**%**
Headache	98
Dizziness	84
Difficulty sleeping	72
Weakness of an upper extremity	69
Neck pain	67
Numbness/tingling of an upper extremity	62
Fatigue	59
Nausea	58
Shortness of breath	57
Blurred vision	57
Tinnitus	56
Difficulty swallowing	54
Weakness of a lower extremity	52

Table: 13 symptoms were reported by more than 50 % of the 265 participating patients with Chiari I malformation in the study by Mueller and Oro' [1]

Syringomyelia

- Fluid-filled cavities (*syrinxes*) develop in spinal cord.
- May cause irreversible nerve damage.
- Estimated 70% of syringomyelia related to hindbrain malformations.
- $30 - 50\%$ of *symptomatic* Chiari I patients develop syrinx.

CSF flow

Cerebrospinal fluid (CSF) flows in the subarachnoid space (SAS) in the brain and spinal column.

- Studies show that Chiari I results in abnormal CSF flow.
  - Velocity
  - Pressure
- Believed to be a possible cause for symptoms and syringomyelia.

The spinal cord

- Part of the central nervous system.
- Encased in the spinal column.
- CSF flows past the spinal cord.
- Cylindrical in shape.
- Made up of grey and white matter.

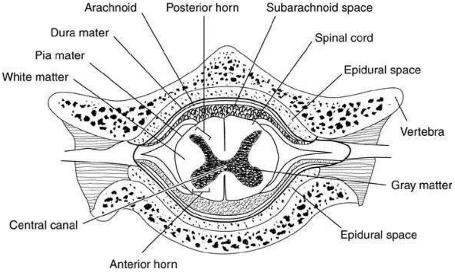

Outline

Simulation scenario

- Anatomically accurate geometry.

- Spinal cord segment from sheep (3.4cm).

Simulation scenario

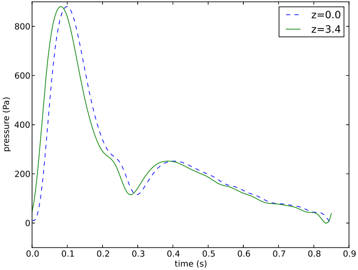

- Measured pressure variation from Chiari patient.
- Pressure modelled as travelling wave,

$$p(z,t) = p_0(z+ct). \quad (1)$$

Outline

- Medical backgound
- Simulation scenario
- Mathematical models
- Discretization
- Implementation
- Simulation results
- Conclusions

Governing equations

Equations for elasticity,

$$-\nabla \cdot \sigma = f, \text{ in } \Omega, \tag{2a}$$
$$u = u_D, \text{ on } \Gamma_D, \tag{2b}$$
$$\sigma \cdot n = g, \text{ on } \Gamma_N. \tag{2c}$$

Neumann BC: Simulates the applies pressure,

$$\sigma \cdot n = -p \cdot n.$$

Dirichlet BC: Constraints on top and bottom boundaries.

- $u_D = 0$.
- $u_D = u_z = 0$.

Constitutive relationships

Stress vs. strain

- $\sigma = \sigma(u(x))$: The stress tensor.
- $\varepsilon = \varepsilon(u(x))$: The strain tensor, defined by

$$\varepsilon = \frac{1}{2}\left(\nabla u + (\nabla u)^T\right). \tag{3}$$

Constitutive relationship: σ expressed in terms of ε.

Linear, isotropic materials.

Constitutive relationships

Linear elasticity

Stress-strain relationship given by

$$\sigma = 2\mu\varepsilon + \lambda \mathrm{tr}(\varepsilon) I. \tag{4}$$

μ, λ: Lamé parameters, known in terms of E (Young's modulus) and ν (Poisson ratio).

Constitutive relationships

Linear viscoelasticity

Stress-strain relationship from spring-dashpot combinations.

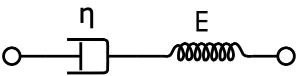

Figure: Maxwell

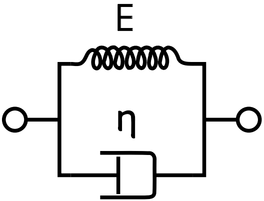

Figure: Kelvin-Voigt

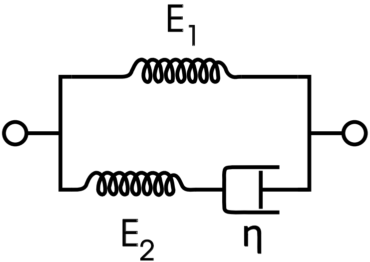

Figure: Standard linear solid (SLS)

Constitutive relationships

Linear viscoelasticity – SLS

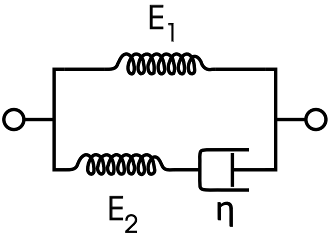

Figure: Standard linear solid (SLS)

Constitutive relationship given by

$$\sigma + \tau_\varepsilon \dot{\sigma} = E_1(\varepsilon + \tau_\sigma \dot{\varepsilon}), \tag{5}$$

where $\tau_\varepsilon = \frac{\eta}{E_2}$ and $\tau_\sigma = \eta \frac{E_1+E_2}{E_1 E_2}$.

Constitutive relationships

Linear viscoelasticity – SLS

Rewritten on integral form:

$$\sigma(t) = D(0)\varepsilon(t) - \int_0^t D_s(t-s)\varepsilon(s)ds, \tag{6}$$

where

$$D(t) = E_1 + E_2\, e^{-t/\tau}. \tag{7}$$

Constitutive relationships

Linear viscoelasticity – SLS (2D/3D)

Extending to 2D/3D,

$$D(t)\varepsilon(t) = 2\mu(t)\varepsilon(t) + \lambda(t)\mathrm{tr}(\varepsilon(t))I, \qquad (8)$$

$$D_s(t-s)\varepsilon(s) = 2\mu_s(t-s)\varepsilon(s) + \lambda_s(t-s)\mathrm{tr}(\varepsilon(s))I, \qquad (9)$$

where

$$\mu(t) = \mu_1 + \mu_2\, e^{-t/\tau},$$
$$\lambda(t) = \lambda_1 + \lambda_2\, e^{-t/\tau}.$$

$\lambda(t) = C\mu(t)$ gives constant Poisson ratio.

$2\mu_1 = E_1$, $2\mu_2 = E_2$.

Parameter values

Constitutive relationship	E_1(Pa)	E_2(Pa)	η(Pa s)	E(Pa)	ν
SLS	0.84×10^3	2.03×10^3	6.7	–	–
SLS*	0.21×10^5	0.53×10^5	1.7×10^2	–	–
Lin. elast	–	–	–	1.6×10^4	0.479
Lin. elast*	–	–	–	6.5×10^2	0.479

Table: Summary of the parameter values selected from the literature.
*:Calculated values.

Outline

Systems to be discretized

Recall:

$$
\begin{aligned}
-\nabla \cdot \sigma &= f, \text{ in } \Omega, \\
u &= u_D, \text{ on } \Gamma_D, \\
\sigma \cdot n &= g, \text{ on } \Gamma_N.
\end{aligned}
$$

Linear elasticity:

$$\sigma = 2\mu\varepsilon + \lambda \mathrm{tr}(\varepsilon) I.$$

Linear viscoelasticity:

$$\sigma(t) = D(0)\varepsilon(t) - \int_0^t D_s(t-s)\varepsilon(s)ds.$$

Variational formulations

Linear elasticity

$$a(u, v) = L(v), \ \ \forall\, v \in V,$$

$$a(u, v) := \int_\Omega 2\mu\varepsilon : \nabla v \ d\Omega + \int_\Omega \lambda \mathrm{tr}(\varepsilon) I : \nabla v \ d\Omega,$$

$$L(v) := \int_\Omega f \cdot v \ d\Omega + \int_{\Gamma_N} g \cdot v \ d\Gamma.$$

Fully discrete:

$$a(u_i^h, v) = L(v), \ \ \forall\, v \in \hat{V}^h$$

Fully discrete schemes

Linear viscoelasticity

$$b(t,t;u(t),v) - \int_0^t c(t,s;u(s),v)\ ds = L(v), \ \ \forall\, v \in V,$$

$$b(t,t;u,v) = \int_\Omega D(0)\varepsilon(t) : \nabla v\ d\Omega,$$

$$c(t,s;u,v) = \int_\Omega D_s(t-s)\varepsilon(s) : \nabla v\ d\Omega,$$

Fully discrete:

$$b(t_i,t_i;u_i^h,v) - \frac{\Delta t}{2} c(t_i,t_i;u_i^h,v)$$

$$= L(v) + \frac{\Delta t}{2} c(t_i,t_0;u_0^h,v) + \Delta t \sum_{j=1}^{i-1} c(t_i,t_j;u_j^h,v), \ \ \forall\, v \in \hat{V}^h$$

Efficient scheme for viscoelasticity

Replace sum term:

$$\sum_{j=1}^{i-1} c(t_i, t_j; u_j^h, v) = e^{-(t_i - t_{i-1})/\tau} \sum_{j=1}^{i-2} c(t_{i-1}, t_j; u_j^h, v) + c(t_i, t_{i-1}; u_{i-1}^h, v). \tag{10}$$

Testing the efficient scheme

	Trapezoidal		Efficient		
Δt	e_h	rate	e_h	rate	Difference
1.00E-01	7.938E-04	–	7.938E-04	–	0.0
5.00E-02	1.735E-04	2.19	1.735E-04	2.19	2.07E-17
2.50E-02	4.067E-05	2.09	4.067E-05	2.09	4.76E-18
1.25E-02	9.852E-06	2.05	9.852E-06	2.05	4.67E-17
6.25E-03	2.425E-06	2.02	2.425E-06	2.02	8.34E-17
3.13E-03	6.015E-07	2.01	6.015E-07	2.01	3.55E-18
1.56E-03	1.498E-07	2.01	1.498E-07	2.01	9.79E-16
7.81E-04	3.738E-08	2.00	3.738E-08	2.00	3.95E-16

Table: Comparing errors in the solution for trapezoidal sum and efficient sum (10).

Testing the efficient scheme

Speedup:

	Time taken (s)
Trapezoidal	1.294
Efficient	0.017
Speedup	74.6

Table: Comparing time taken to obtain solution when using trapezoidal sum and efficient sum (10).

Boundary conditions

Γ_1, Γ_2: top and bottom boundary respectively.

- $u_z = 0$ on Γ_1, Γ_2
- No-rotation BC: $u \cdot e_\theta = 0$ on Γ_1, Γ_2, where

$$e_\theta = \begin{pmatrix} \frac{-(y_0+y)}{r} \\ \frac{x_0+x}{r} \\ 0 \end{pmatrix},$$

  x_0, y_0: points, $r = \sqrt{(x_0 + x)^2 + (y_0 + y)^2}$.

- $u = 0$ on point in Γ_1, Γ_2.

Boundary conditions

Weakly enforcing no-rotation condition

Using Nitsche's method, variational form: Find $u \in V$ such that

$$\begin{aligned}
&\int_{\Omega} \sigma(u) : \nabla v \, d\Omega + \frac{\gamma}{h_E} \int_{\Gamma_{1,2}} (u \cdot e_\theta)(v \cdot e_\theta) \, d\Gamma \\
&\quad - \int_{\Gamma_{1,2}} (\sigma(u) \cdot n \cdot e_\theta)(v \cdot e_\theta) \, d\Gamma - \int_{\Gamma_{1,2}} (\sigma(v) \cdot n \cdot e_\theta)(u \cdot e_\theta) \, d\Gamma \\
&= \int_{\Omega} f \cdot v \, d\Omega + \int_{\Gamma_N} g \cdot v \, d\Gamma + \frac{\gamma}{h_E} \int_{\Gamma_{1,2}} (u \cdot e_\theta)(v \cdot e_\theta) \, d\Gamma \\
&\quad - \int_{\Gamma_{1,2}} (\sigma(v) \cdot n \cdot e_\theta), (u_0 \cdot e_\theta) \, d\Gamma, \;\; \forall \, v \in \hat{V},
\end{aligned} \tag{11}$$

Outline

- Medical backgound
- Simulation scenario
- Mathematical models
- Discretization
- **Implementation**
- Simulation results
- Conclusions

Implementation

- Python
- FEniCS
  - PETSc
    - Direct LU solver (testing)
    - Krylov solver: GMRES with AMG preconditioner (simulations)
- Object oriented approach

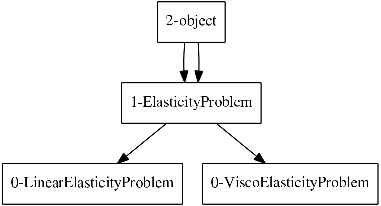

Verifying the implementations

Linear elasticity

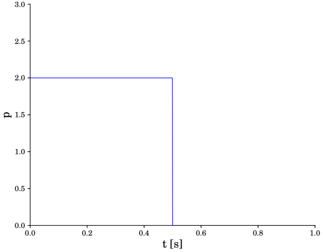

(a) Applied pressure

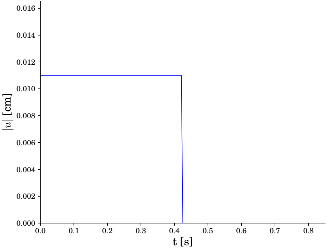

(b) Displacement

Figure: (a) Pressure variation over time, and (b) Resulting displacement over time in a chosen point in the mesh from simple pressure simulation using linear elasticity solver on unit square geometry (2D).

Verifying the implementations

Linear elasticity

	Degree 1		Degree 2	
h	e	rate	e	rate
2.50E-01	1.53E-01	–	2.33E-03	–
1.25E-01	4.46E-02	1.78	2.78E-04	3.07
6.25E-02	1.17E-02	1.93	3.41E-05	3.03
3.12E-02	2.97E-03	1.98	4.22E-06	3.01
1.56E-02	7.46E-04	1.99	5.26E-07	3.01
7.81E-03	1.87E-04	2.00	6.56E-08	3.00

Table: Errors in the numerical solution u for linear elasticity, when compared to a manufactured exact solution u_e, for elements of degrees 1 and 2 in 2D using direct LU solver.

Verifying the implementations
Linear viscoelasticity

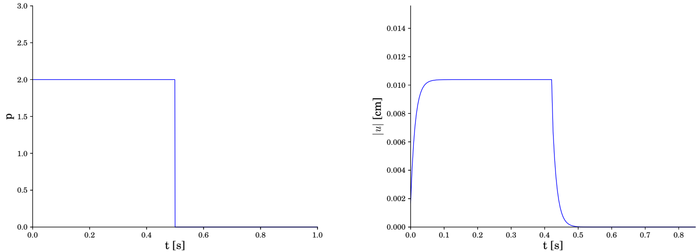

(a) Applied pressure **(b)** Displacement

Figure: (a) Pressure variation over time, and (b) Resulting displacement over time in a chosen point in the mesh from simple pressure simulation using linear viscoelasticity solver on unit square geometry (2D).

Verifying the implementations

Linear viscoelasticity

$\Delta t \setminus h$	*3.54E-01*	*1.77E-01*	*8.84E-02*	*4.42E-02*	*2.21E-02*	*1.10E-02*
2.00E-02	**4.19E-03**	3.96E-03	5.64E-03	6.09E-03	**6.21E-03**	**6.23E-03**
1.00E-02	7.90E-03	**1.18E-03**	9.64E-04	1.38E-03	**1.49E-03**	**1.51E-03**
5.00E-03	8.91E-03	2.12E-03	**3.10E-04**	2.40E-04	**3.43E-04**	**3.68E-04**
2.50E-03	9.16E-03	2.37E-03	5.42E-04	**7.87E-05**	**5.98E-05**	**8.37E-05**
1.25E-03	9.22E-03	2.44E-03	6.07E-04	1.37E-04	**1.98E-05**	-*
1.00E-04	9.24E-03	2.46E-03	6.29E-04	1.58E-04	**3.95E-05**	-*
5.00E-05	**9.24E-03**	**2.46E-03**	**6.29E-04**	**1.58E-04**	**3.96E-05**	-*

Table: Errors in the numerical solution for linear viscoelasticity (SLS model), when compared to a manufactured exact solution, for elements of degree 1 in 2D using direct LU solver.

Verifying the implementations

Linear viscoelasticity

$\Delta t \setminus h$	*3.54E-01*	*1.77E-01*	*8.84E-02*	*4.42E-02*	*2.21E-02*
2.00E-02	**6.25E-03**	6.25E-03	6.25E-03	6.25E-03	**6.25E-03**
1.00E-02	1.53E-03	**1.53E-03**	1.53E-03	1.53E-03	**1.53E-03**
5.00E-03	3.85E-04	3.80E-04	**3.79E-04**	3.79E-04	**3.79E-04**
2.50E-03	1.06E-04	9.51E-05	9.47E-05	**9.47E-05**	**9.47E-05**
1.25E-03	4.61E-05	2.45E-05	2.37E-05	2.37E-05	**2.37E-05**
1.00E-04	3.69E-05	5.13E-06	6.89E-07	1.75E-07	**1.52E-07**
5.00E-05	**3.69E-05**	**5.12E-06**	**6.70E-07**	**9.37E-08**	**3.94E-08**

Table: Errors in the numerical solution for linear viscoelasticity (SLS model), when compared to a manufactured exact solution, for elements of degree 2 in 2D using direct LU solver.

Outline

- Medical backgound
- Simulation scenario
- Mathematical models
- Discretization
- Implementation
- Simulation results
- Conclusions

Simulations

Overview of the models

	SLS			
	E_1(Pa)	E_2(Pa)	η(Pa s)	C
Model 1	0.84×10^3	2.03×10^3	6.7	22.8 (0.479$*$)
Model 2	0.21×10^5	0.53×10^5	1.7×10^2	22.8 (0.479$*$)
Model 3	0.84×10^3	2.03×10^3	13.4	22.8 (0.479$*$)
Model 4	0.84×10^3	2.03×10^3	6.7	0.0 (0.0$*$)
	Linear elasticity			
	E(Pa)	ν		
Model 5	1.6×10^4	0.479	–	–
Model 6	6.5×10^2	0.479	–	–

Table: Summary of the parameters to be used in simulations. *ν, defined implcitly through C.

Viscoelastic results

Visual plot: Models 1 and 3

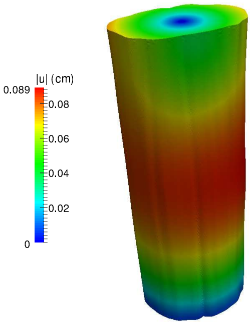

(a) Model 1

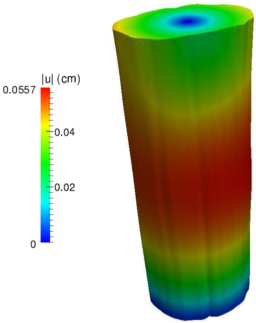

(b) Model 3

Figure: Visual comparison of Model 1 and Model 3 at $t = 0.075$s. The displacement patterns are similar for Models 1 and 3, while the magnitudes of the displacement differ slightly.

Viscoelastic results

Line plot: Models 1 and 3

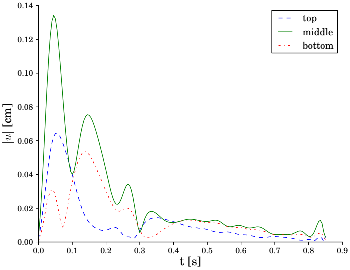

(a) Model 1

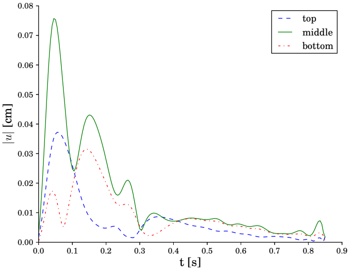

(b) Model 3

Figure: Displacement magnitude over time for chosen points in the geometry for Model 1 and Model 3. The two plots show the similar qualitative behavior, but differ in magnitude.

Viscoelastic results

Visual plot: Models 1 and 4

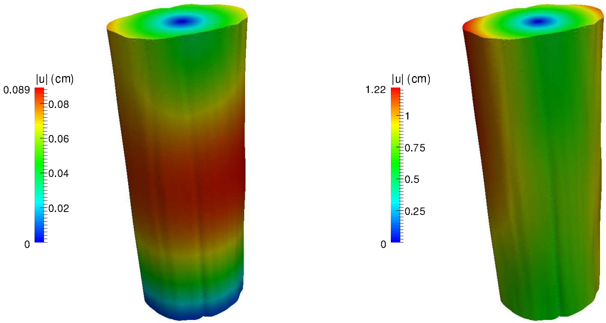

(a) Model 1 **(b)** Model 4

Figure: Visual comparison of Model 1 and Model 4 at $t = 0.075$s. The displacement patterns are drastically different for Models 1 and 4, as are the magnitudes of the displacement.

Viscoelastic results

Line plot: Models 1 and 4

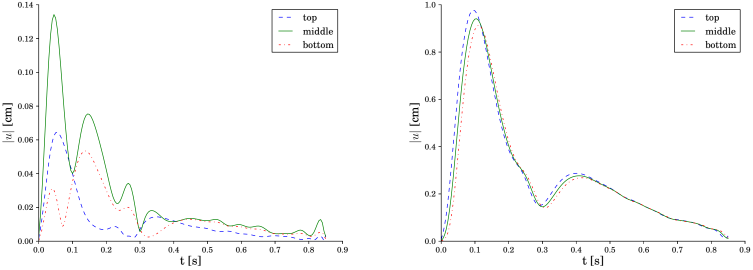

(a) Model 1 **(b)** Model 4

Figure: Displacement magnitude over time for chosen points in the geometry for Model 1 and Model 4. The two plots differ both in qualitative behavior and in magnitude.

Viscoelastic results

Line plot: Model 1 over 4 cycles

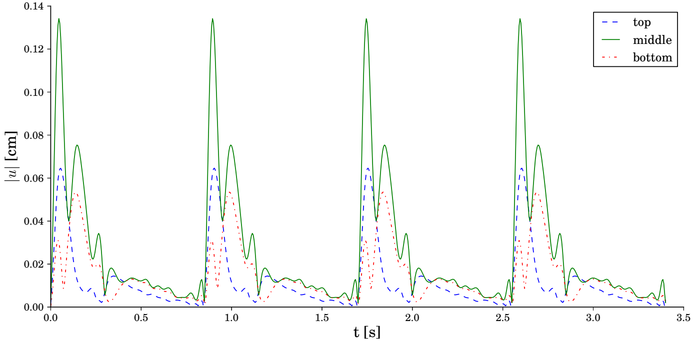

Figure: Displacement in the selected points over four cycles ($T = 3.4$s).

Viscoelastic results

Peak displacements over time: Model 1

Cycle	$u_{T,max}$(cm)	$u_{M,max}$(cm)	$u_{B,max}$(cm)
1	0.064560	0.134180	0.0534309
2	0.064612	0.134151	0.0534311
3	0.064609	0.134119	0.0534312
4	0.064609	0.134119	0.0534312

Table: Peak displacements for the points x_T, x_M and x_B for each cycle, using Model 1 with $T = 3.4$. The difference in the peak displacements over four cycles is in the order of 1×10^{-7}m for each of the points.

Comparing with linear elasticity

Visual plot: Models 1 and 6

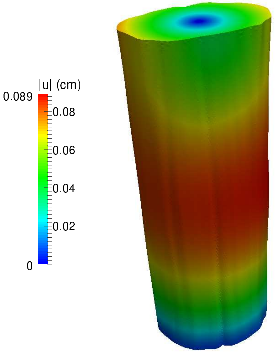

(a) Model 1

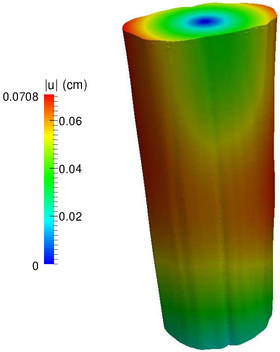

(b) Model 6

Figure: Visual comparison of Model 1 and Model 6 at $t = 0.075$s.

Comparing with linear elasticity

Line plot: Models 1 and 6

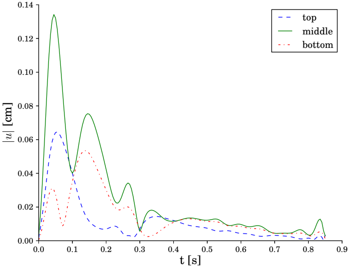

(a) Model 1

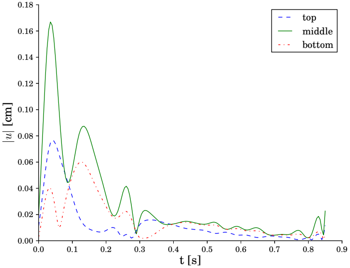

(b) Model 6

Figure: Displacement magnitude over time for a chosen point in the geometry for Model 1 and Model 6. The two curves show the similar qualitative behavior, but differ in magnitude.

Comparing with linear elasticity

Time taken to reach peak displacement: Models 1 and 6

	Reaches peak after (s)	
Point	Model 1	Model 6
x_T	0.055	0.04
x_M	0.045	0.035
x_B	0.14	0.125

Table: Time taken to reach peak displacement for the chosen points in Model 1 and Model 6.

Comparing with linear elasticity

Visual plot: Models 2 and 5

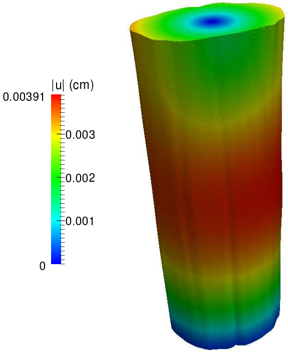

(a) Model 2

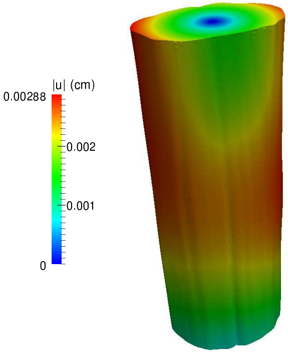

(b) Model 5

Figure: Visual comparison of Model 2 and Model 5 at $t = 0.075$s.

Comparing with linear elasticity

Line plot: Models 2 and 5

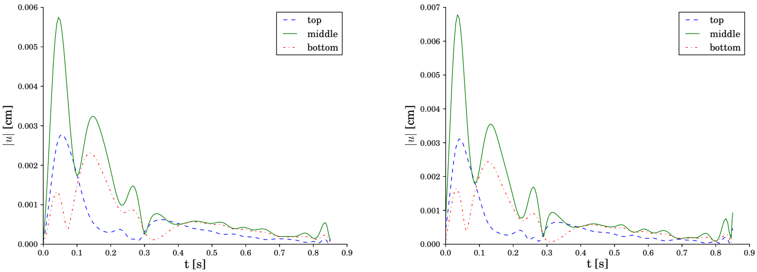

(a) Model 2 **(b)** Model 5

Figure: Displacement magnitude over time for a chosen point in the geometry for Model 2 and Model 5. The two curves show the similar qualitative behavior, but differ in magnitude.

Comparing with linear elasticity

Peak displacements over time: Model 6

Cycle	$u_{T,max}$(cm)	$u_{M,max}$(cm)	$u_{B,max}$(cm)
1	0.0765298	0.166881	0.0600790
2	0.0765298	0.166881	0.0600790
3	0.0765298	0.166881	0.0600790
4	0.0765298	0.166881	0.0600790

Table: Peak displacements for the points x_T, x_M and x_B for each cycle, using Model 6 with $T = 3.4$. There is no difference in the magnitude of the peak displacement for each cycle.

Comparing with linear poro

Visual comparison: Poroelastic, linear elastic, linear viscoelastic

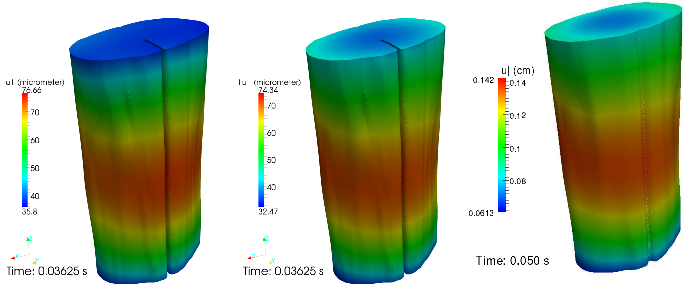

(a) Poroelastic [2] **(b)** Linear elastic [2] **(c)** SLS, Model 1

Figure: Comparison of results from Støverud et. al. [2] with viscoelastic results using Model 1. Note that the top and bottom 0.5cm have been cut from the geometry to display the same geometry as Støverud et. al. [2].

Outline

Conclusions

- Difficult to establish parameter values.
- Scaling parameter magnitudes affects displacement magnitudes.
- Changing η – effect on magnitude and behaviour.
- Compressibility important.
- Small but clear viscoelastic effect:
  - Lag, approx 10ms.
  - Varying peak displacement over several cycles, $\approx 10^{-7} - 10^{-8}$m.

Conclusions

- Viscoelastic behaviour similar to linear elastic behaviour.
  - Lag does not seem to be significant.
  - Variation in peak displacements over time appears to decrease over time, not increase.
- Linear viscoelastic model has little or no effect in context of syringomyelia.
- Elastic/viscoelastic models assume solid spinal cord.
- Poroelastic model – fluid flow within spinal cord.

Further work

- Develop standard procedures for obtaining parameter data.
  - Standardized parameter values.
- Obtain patient-specific spinal cord geometry, parameter data and pressure data.
- Test effect of non-linear model.
- Couple with CDF simulations of CSF flow.

Thank you for your attention!

References I

Diane M. Mueller, ND RN and John J. Oro', MD.

Prospective Analysis of Presenting Symptoms Among 265 Patients With Radiographic Evidence of Chiari Malformation Type I With or Without Syringomyelia.

Journal of the American Academy of Nurse Practitioners, 16(3), 2004.

References II

Støverud, Karen H. and Alnæs, Martin and Langtangen, Hans Petter and Haughton, Victor and Mardal, Kent-André.

Effect of pia mater, central canal, and geometry on wave propagation and fluid movement in the cervical spinal cord.

Manuscript submitted for publication, 2014.